

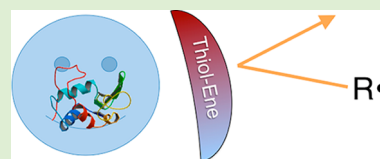
Thiol–Ene Photopolymerizations Provide a Facile Method To Encapsulate Proteins and Maintain Their Bioactivity

Joshua D. McCall[†] and Kristi S. Anseth^{*,†,‡}

[†]Department of Chemical and Biological Engineering and the BioFrontiers Institute, University of Colorado at Boulder, Boulder, Colorado, 80303, United States

[‡]Howard Hughes Medical Institute, University of Colorado at Boulder, Boulder, Colorado, 80303, United States

ABSTRACT: Photoinitiated polymerization remains a robust method for fabrication of hydrogels, as these reactions allow facile spatial and temporal control of gelation and high compatibility for encapsulation of cells and biologics. The chain-growth reaction of macromolecular monomers, such as acrylated PEG and hyaluronan, is commonly used to form hydrogels, but there is growing interest in step-growth photopolymerizations, such as the thiol–ene “click” reaction, as an alternative. Thiol–ene reactions are not susceptible to oxygen inhibition and rapidly form hydrogels using low initiator concentrations. In this work, we characterize the differences in recovery of bioactive proteins when exposed to similar photoinitiation conditions during thiol–ene versus acrylate polymerizations. Following exposure to chain polymerization of acrylates, lysozyme bioactivity was approximately 50%; after step-growth thiol–ene reaction, lysozyme retained nearly 100% of its prereaction activity. Bioactive protein recovery was enhanced 1000-fold in the presence of a thiol–ene reaction, relative to recovery from solutions containing identical primary radical concentrations, but without the thiol–ene components. When the cytokine TGF β was encapsulated in PEG hydrogels formed via the thiol–ene reaction, full protein bioactivity was preserved.



INTRODUCTION

Poly(ethylene glycol) (PEG) is utilized for a number of biomaterial applications, including antithrombotic and antifouling surfaces,^{1,2} implantable medical devices,^{3,4} drug delivery,^{3,5–7} and three-dimensional cell scaffolds.^{8–10} The hydrophilic nature of PEG minimizes nonspecific interactions with many biomacromolecules, providing a material platform that is highly resistant to protein adsorption.^{11,12} PEG is easily modified with functional end groups that can be subsequently cross-linked to form covalently linked networks. There is growing interest in the use of PEG hydrogels formed from such reactions, especially photoinitiated cross-linking reactions that can be performed in the presence of cells or biomolecules *in situ*. In the case of cell encapsulation, a variety of cytocompatible photopolymerization conditions have been identified that proceed at physiological temperature and osmolarity,^{13–16} but conditions for encapsulation of proteins while maintaining activity are more stringent.^{17,18}

A common approach to forming PEG hydrogels is the chain polymerization of multi(meth)acrylated PEG monomers. This acryl homopolymerization proceeds to high conversion in aqueous environments, with rapid gel formation and development of a network structure characteristic of radically mediated chain growth polymerizations.^{19,20} Photoinitiation is often used to form PEG gels, which allows spatial and temporal control of the polymerization process. Hydrogel formation using photoinitiated polymerization of (meth)acrylated PEG monomers is particularly favorable for the encapsulation of cells, proteins, and other biologically relevant molecules, as this approach allows for cytocompatible reaction temperature and facile maintenance of sterile conditions.¹⁴ Furthermore, a number of

water-soluble photoinitiating species are commercially available, and the reaction exhibits low cytotoxicity at the wavelengths and light dosages typically required for hydrogel formation.^{13,14} However, the photoencapsulation of proteins and biologics can be more challenging and appropriate reaction conditions more difficult to identify.^{17,18,21,22}

While robust, the use of a radically mediated polymerizations poses additional challenges when forming hydrogels via solution polymerization of (meth)acrylated monomers. For instance, radical mediated chain-growth polymerizations are susceptible to oxygen inhibition,^{23–25} which results in longer polymerization times and requires increased irradiation dosing. Further, when used for encapsulation of biomacromolecules, the increased radical generation, lifetime, and exposure time can lead to undesired side effects, namely, damage of the encapsulant.^{17,18} A number of amino acids have reported antioxidant potential, including tyrosine, tryptophan, and cysteine among others,^{26,27} although cysteine is typically present in an oxidized state in the form of disulfide bridges, which has a lowered antioxidant potential.²⁸ Radical transfer from propagating polymeric chains to biomacromolecules can result in changes to protein secondary and tertiary structure,¹⁷ chain scission,^{27,29} or protein–polymer conjugation. Several approaches have been shown to ameliorate this protein damage in (meth)acrylate chain-growth reactions. For instance, higher concentrations of acrylate monomer are effective in protecting lysozyme during photoinitiated polymerization,¹⁷ and peptide

Received: April 27, 2012

Revised: June 26, 2012

Published: June 29, 2012

affinity ligands included in prepolymer solutions protect the cytokine TGF β during encapsulation in PEG diacrylate hydrogels.¹⁸ While much effort has focused on strategies to minimize damage to encapsulated biologics during photo-initiated radical polymerization of PEGs, we sought to investigate the potential benefits of using different PEG precursors that undergo a radical mediated photopolymerization.

In particular, there is a growing interest in “click” based thiol–ene photopolymerization.^{30–33} The thiol–ene reaction proceeds via a radical-mediated mechanism, but by proper choice of the ene functionality, gel formation occurs via a step-growth mechanism. As a result, even with similar photo-initiation conditions, the radical concentrations and lifetimes can be substantially different during the evolution of PEG gels formed via acrylate chain polymerization versus thiol–ene step polymerizations. For example, PEG functionalized with terminal norbornene groups and reacted with bis(thiol) cross-linkers has been successfully copolymerized through photo-initiation to create hydrogel platforms for a number of biomaterials applications, including encapsulation of fibroblasts,¹⁰ pancreatic β cells,³⁴ human mesenchymal stem cells,³⁵ primary valvular interstitial cells,³⁶ and therapeutic proteins.³⁷ The thiol–ene reaction involves two steps: first, an initiator radical is transferred to a thiol, creating a thiyl radical that propagates across a carbon–carbon double bond; second, the carbon-radical rapidly undergoes chain-transfer to a new thiol, regenerating the thiyl species and allowing for a cycle of coupling reactions that form the macroscopic network (Scheme 1B). Relative to (meth)acrylate chain growth, the thiol–ene

improve protein bioactivity during encapsulation. In this work, we systematically compare protein activity during photo-initiated polymerization of PEG precursors utilizing two polymerization schemes: (i) acrylate chain-growth and (ii) thiol–ene step-growth reactions. In both the cases, polymerizations are photoinitiated using a water-soluble initiator, lithium acylphosphinate (LAP), and conducted in the presence of two proteins, lysozyme and TGF β , to study the protein bioactivity during these radically mediated photopolymerizations. We investigate loss in protein bioactivity as a result of exposure to photoinitiated radicals and characterize the differences in bioactivity when acrylates versus thiol–ene functional groups are polymerized using the same initial functional group concentrations. We show that at high extents of reaction, the thiol–ene step-growth reaction affords significantly higher levels of recovery of bioactive protein relative to that observed following chain-growth acrylate homopolymerization. We correlate loss of protein activity to the concentration of radicals generated and show that, during a thiol–ene polymerization, protein activity is preserved over a much broader range of photopolymerization conditions.

EXPERIMENTAL SECTION

Materials. All chemicals were purchased from Sigma-Aldrich unless noted otherwise.

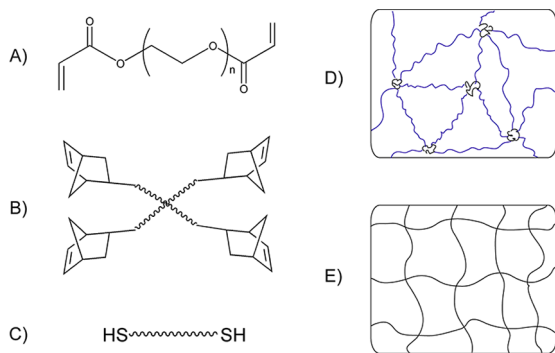
Synthesis of 4-Arm PEG Norbornene. 4-Arm PEG norbornene (PEG-4-NB) was synthesized as detailed elsewhere.¹⁰ Briefly, 5-norbornene 2-carboxylic acid was added at 10 \times excess (basis: PEG hydroxyl groups), with 5 \times excess dicyclohexylcarbodiimide in dichloromethane, and the solution was stirred for 30 min at room temperature. Separately, 4-arm PEG (M_n 10000) (JenKem U.S.A.) was dissolved in DCM, with 5 \times pyridine and 0.5 \times 4-(dimethylamino)pyridine (DMAP) and then added to the DCC/norbornene solution. The reaction mixture was stirred overnight at room temperature under argon. The product was precipitated into ice-cold ethyl ether and subsequently washed using Soxhlet extraction into ethyl ether.

Synthesis of PEG Diacrylate. Linear PEG diacrylate was synthesized as detailed previously.⁴¹ Briefly, PEG (M_n 4600) was dissolved in toluene and reacted with 4 \times acryloyl chloride (basis: PEG hydroxyls) in the presence of 4 \times triethylamine. The mixture was stirred at room temperature overnight under argon. Product was washed in DCM and precipitated in cold ethyl ether.

In Situ Dynamic Rheology during Photopolymerization. Rheometrical measurements were carried out on an Ares TA rheometer using a parallel plate geometry. Hydrogels were formed using 10 wt % solutions of PEG-4-NB (M_n 10000) reacted with linear PEG dithiol (Sigma) or PEGDA (M_n 4600). Approximately 30 s after beginning measurement, UV light ($\lambda = 365$ nm, $I_0 = 10$ mW/cm²) was introduced to the monomer solutions through a quartz plate, and modulus measurements were recorded in situ at 10% strain, 100 rad/s. These settings were used after confirming that they were within the linear range, using strain sweeps on monomer solutions and the final cross-linked polymer.

Lysozyme Monomer Photopolymerization Studies. All monomer solutions were prepared with lysozyme (Worthington Biochemical) at a concentration of 1 μ M, and photopolymerization was initiated using an Omnicure lamp ($\lambda = 365$ nm) under optically thin conditions (100 μ L monomer/sample). Nongelling acrylate polymerizations were conducted using PEG monoacrylate ($M_n = 2000$; Monomer-Polymer and Dajac Laboratories) at a concentration of 40 mM in PBS, with 1 mM LAP initiator. Four-arm PEG norbornene ($M_n = 10000$) was reacted at 10 mM (40 mM norbornene) with a stoichiometric cysteine concentration to create a nongelling thiol–ene monomer system. Thiol–ene polymerization reactions were initiated with 0.1, 1, or 10 mM LAP. Following photopolymerization, protein/polymer solutions were assayed for enzymatic activity as described below.

Scheme 1. Monomer and Polymer Structure^a



^a(A) PEG diacrylate, (B) PEG 4-arm norbornene, and (C) PEG dithiol. Upon polymerization, PEG diacrylate forms a chain-growth network as depicted in (D), while the thiol–ene reaction forms a step-growth network (E).

reaction is less susceptible to oxygen inhibition³⁰ and differs in both the reactivity of the propagating radical species and the radical lifetime. While many measurements of acryl radical concentrations during photopolymerization have been reported,^{38–40} no such measurement has yet been published for thiol–ene polymerizations and it is often implied that part of the reason for this lack of quantification is the very low radical concentrations.³⁰ Further, the rapid polymerization of thiol–norbornene cross-linked polymers at physiological conditions makes these monomer systems an excellent choice for many in situ forming hydrogel applications.

We speculated that the lower radical concentration and rapid polymerization of the thiol–ene step-growth reaction might

Lysozyme Bioactivity Assay. Lysozyme from chicken embryo (Worthington Biochemical) was reconstituted at 50 mg/mL in deionized water and further diluted to an appropriate working range (150–450 U/mL) in deionized water. The substrate micrococcus lysodeiktuus (Worthington Biochemical) was reconstituted in deionized water at 0.6–1.0 mg/mL. For measurements of native bioactivity, solutions of lysozyme and substrate were mixed at a 1:1 ratio and changes in absorbance at 450 nm were measured on a Biotek Hybrid H1 spectrophotometer. Changes in absorbance were plotted versus time and correlated to changes in relative bioactivity.

TGF β Bioactivity Assay. TGF β bioactivity was quantified as described elsewhere,⁴² using a mink lung epithelial cell line (PE.25) permanently transfected with a luciferase reporter for SMAD2 gene activity such that the cells produce luciferase upon culture with bioactive TGF β . Briefly, PE.25 cells were plated in 24-well TCPS plates (100000 cells/well) in serum-free DMEM and incubated overnight at 37 °C, 5% CO₂ prior to culture with monomer solutions.

Nongelling monomer solutions were formulated using either PEG monoacrylate or PEG 4-norbornene/cysteine (500 μ L/sample). Each monomer solution was prepared to yield 40 mM reactive group concentration and TGF β (Peprotech) at 20 nM. Photopolymerization was initiated using 1 mM LAP at $I_0 = 10$ mW/cm² ($\lambda = 365$ nm) in a sterile hood. Prior to and following photopolymerization, 100 μ L of the protein/polymer solution was diluted 1:1000 in serum-free DMEM media, and PE.25 cells were cultured in such for 18 h. Cells were lysed and analyzed using Glo-Lysis reagents (Promega), and luciferase production was quantified using a Biotek Hybrid H1 spectrophotometer.

Encapsulation and Recovery of Model Proteins from Cross-Linked Thiol–Ene Hydrogels. Monomer solutions were formulated with 1 mM LAP, 4-arm PEG norbornene, and linear PEG dithiol ($M_n = 1500$). Lysozyme, chymotrypsinogen (Worthington Biochemical), collagenase 3 (Worthington Biochemical), and bovine serum albumin were encapsulated at 100 μ g/gel (gel volume = 50 μ L), and human serum was encapsulated at 4% v/v (gel volume of 50 μ L). Gels were formed by exposing the solutions to $I_0 = 10$ mW/cm² ($\lambda = 365$ nm) for 5 s, then immediately placed into 2 mL of PBS. After 24 h incubation at 4 °C, the supernatant was assayed for protein concentration using MicroBCA (Pierce), as per the manufacturer's instructions.

Encapsulation and Recovery of Bioactive TGF β from Cross-Linked Thiol–Ene Hydrogels. A monomer solution of 4-arm PEG norbornene ($M_n = 10000$), linear PEG dithiol ($M_n = 2000$), 1 mM LAP, and 20 nM TGF β was used to form cross-linked PEG hydrogels. A total of 100 μ L of this monomer solution was cross-linked by exposure to light ($I_0 = 10$ mW/cm², $\lambda = 365$ nm) for 10 s and immediately placed in 10 mL of serum-free medium. Alternatively, 100 μ L of a monomer solution with 1 mM LAP and 20 nM TGF β was placed directly into 10 mL of serum-free medium (in the absence of polymerization). Both media were incubated overnight at 37 °C, 5% CO₂, and then incubated with PE.25 cells for 18 h under sterile conditions. The cells were lysed and analyzed for luciferase activity as described above.

Statistical Analysis. All data were plotted and analyzed using Graphpad Prism 5.0 software. Error bars are plotted as standard error measurement for three replicate conditions, unless otherwise noted.

RESULTS AND DISCUSSION

Network Formation of Thiol–Ene and Acrylate Hydrogels. To compare the formation of hydrogel networks prepared from acrylate and thiol–ene reactions on protein activity, some measure of the light dosage needed to completely react the monomer functional groups via the respective mechanisms was required. While direct monitoring of functional group conversion with spectroscopic methods was difficult because of their dilute concentration, we found in situ rheology under UV exposure to be a highly sensitive method to monitor shear modulus development during

photopolymerization. Others^{43–45} have shown that the plateau in the modulus correlates well with approximate reaction times for complete photopolymerization of hydrogels. Figure 1A

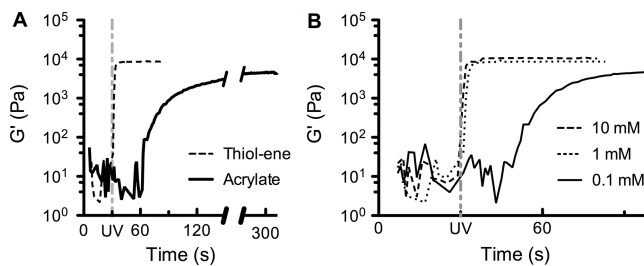


Figure 1. In situ rheology during photopolymerization shows evolution of mechanical properties for hydrogels formed via chain-growth acrylate and step-growth thiol–ene polymerizations. (A) Hydrogel formation for polymerization initiated at 10 mW/cm² ($\lambda = 365$ nm), in the presence of 1 mM LAP. For equal initial functional group concentrations (40 mM), the thiol–ene reaction reached a maximum shear modulus of 10 kPa in less than ten seconds. (B) For a constant thiol–ene initial functional group concentration of 40 mM, polymerization was initiated using an intensity of 10 mW/cm² ($\lambda = 365$ nm), while the LAP initiator concentration was varied from 0.1 to 10 mM. A total of 10 and 1 mM LAP concentrations promoted complete cross-linking in less than 10 s, but the polymerization was much slower with only 0.1 mM initiator and required \sim 60 s of light exposure for complete gel formation.

shows a plot of shear modulus (G') versus reaction time for monomer solutions irradiated at $I_0 = 10$ mW/cm² ($\lambda = 365$ nm). Initial functional group concentrations for both acrylate and thiol–ene systems were 40 mM, corresponding to an approximate 10 wt % monomer solution. The initial concentrations were set equal to make comparisons between the two systems, as both the reaction time and protein stability depend on the functional group concentration. Both the polymerizations were photoinitiated with LAP at an initial concentration of 1 mM. As observed in Figure 1A, the step-growth thiol–ene reaction proceeds rapidly, achieving a shear modulus on the order of 10 kPa after less than 10 s of light exposure.

In contrast, the diacrylate chain-growth reaction requires over 300 s of light exposure to asymptotically approach a maximum modulus value, although after 180 s, the shear modulus was within \sim 95% of the polymer's final G' of approximately 10 kPa. Further, a significant lag time in elastic modulus evolution was observed (i.e., \sim 30 s) and is likely attributable to oxygen inhibition of the acrylate reaction, which is negligible in thiol–ene reactions.^{30,46} The need to generate more radicals to overcome inhibition can become problematic for radically sensitive applications like cell or protein encapsulation. This is noteworthy, as a hydrogel formed via the thiol–ene necessitates shorter polymerization times, and therefore, fewer photoinitiated radical species are generated (Table 1).

Because the thiol–ene reaction is very rapid at typical photoinitiator concentrations used to make PEG-acrylate gels, we next investigated the effect of LAP initiator concentration on the polymerization time required to form PEG hydrogels using the thiol–ene reaction. By varying the LAP concentration used to photoinitiate the reaction at a constant light intensity ($\lambda = 365$ nm, $I_0 = 10$ mW/cm²), the total time required for reaching a maximum shear modulus can be tuned (Figure 1B).

Table 1. Radicals Generated as a Function of Initiator Concentration and Exposure Time for an Intensity of $I_0 = 10$ mW/cm^{2a}

functional group	[LAP], mM	time to reach 95% of G'_{max} s ^b	total initiator radicals generated, mM ^c
acrylate	1	180	1.82
thiol–ene	0.1	60	0.11
	1	5	0.13
	10	1	0.27

^aTotal initiator radicals generated were calculated using exposure total times determined from in situ rheology during photopolymerization and species balance on the initiator and initiator radicals generated.⁴⁷

^bAs measured using rheology during photopolymerization. ^cAs calculated using $R_i = ((2f\phi'\epsilon_i)/(N_A h\nu))I_0[LAP]_0$, where f is initiator efficiency, ϕ' is the number of radicals formed per photon absorbed, ϵ_i is the initiator molar absorptivity at a given wavelength, I_0 is the incident light intensity, N_A is Avogadro's number, h is Planck's constant, and ν represents the frequency of initiating light. The photoinitiator concentration [LAP] is represented as a function of exposure time.

At both 1 and 10 mM LAP concentration, the thiol–ene hydrogel forms rapidly, and in less than 10 s of UV exposure, G' has reached a maximum of approximately 10 kPa. Only at the lowest initiator concentration tested, 0.1 mM LAP, does the thiol–ene polymerization require significantly longer exposure times of 60 s. Despite this longer exposure time, the 0.1 mM LAP condition still generates a lower total number of radicals than the 1 and 10 mM LAP conditions (Table 1). Interestingly, over 3 orders of magnitude in LAP concentration range, the thiol–ene reaction can be utilized to form hydrogels with lower irradiation doses than that required to form similar PEG diacrylate networks, suggesting the thiol–ene polymerization may be advantageous for encapsulation of proteins or cells with known radical susceptibility.

Loss of Protein Bioactivity from Initiator Radical Species. After determination of the time scale for development of hydrogel networks using acrylate and thiol–ene reactions, it was necessary to determine similar ranges for the time scale and light doses to observe radically mediated protein damage. Lysozyme, an enzyme that lyses the bacterial cell wall as part of the innate immune system, was used as a model for screening protein bioactivity under various reaction conditions. Native lysozyme bioactivity was measured and subsequently used as a benchmark for relative comparison. Solutions of lysozyme were then prepared, including LAP at a concentrations of 0.1 and 1

mM and irradiated with UV light ($\lambda = 365$ nm) at two intensities, 1 and 10 mW/cm², respectively, for a total of 60 s. Results are shown in Figure 2. At the highest light intensity of 10 mW/cm² (Figure 2A), protein inactivation was rapid.

In particular, for the 1 mM LAP condition, 15 s of light exposure resulted in complete loss of protein function. Lowering the LAP concentration to 0.1 mM slowed this protein destruction; after 60 s of exposure, approximately 75% of activity was lost. The total number of radicals generated can be further lowered by reducing the light intensity, as shown in Figure 2B. As expected, when the incident light intensity is reduced to 1 mW/cm², a LAP concentration of 1 mM results in 75% protein inactivation after 60 s of light exposure, because the radicals generated for this condition should be identical to that of $I_0 = 10$ mW/cm² at a LAP concentration of 0.1 mM. For the mildest condition tested, $I_0 = 1$ mW/cm², with LAP at 0.1 mM, 60 s of light dosage resulted in ~25% loss of protein function, signifying that, at lower radical concentrations, lysozyme exhibits some functional stability.

To characterize this protein damage in terms of radicals generated, the four protein activity data sets were plotted as a function of total photoinitiated radicals generated in Figure 2C. The loss of protein activity collapses along a characteristic sigmoidal curve, with a critical threshold of ~0.002 mM radicals. Below this concentration, there is little to no loss of lysozyme function. Above this plateau concentration, relative protein bioactivity rapidly declines, and total loss of bioactivity is achieved above a concentration of ~0.5 mM radicals generated. This is quite interesting to note, as the concentration of dissolved oxygen in acrylic monomer solutions has reported on the order of 0.5–2 mM.^{48,49} One potential cause for this 0.5 mM radical threshold is the formation of reactive oxygen species, effectively consuming primary photogenerated radical species to protein in situ lysozyme.

Protein Damage in the Presence of Photoinitiated Acrylate and Thiol–Ene Polymerizations. Next, solution polymerizations were used to study the loss of lysozyme bioactivity when the protein was present in situ during radically mediated acrylate and thiol–ene reactions. Model formulations were selected to avoid gel formation and allow for ease of protein recovery. Nongelling monomer systems were formulated at 40 mM functional group concentration, approximately equal to those used for hydrogel formation (Figure 1). The acrylate chain-growth reaction was modeled using PEG-monoacrylate, while the thiol–ene reaction was characterized using 4-arm PEG norbornene in conjunction with cysteine, a

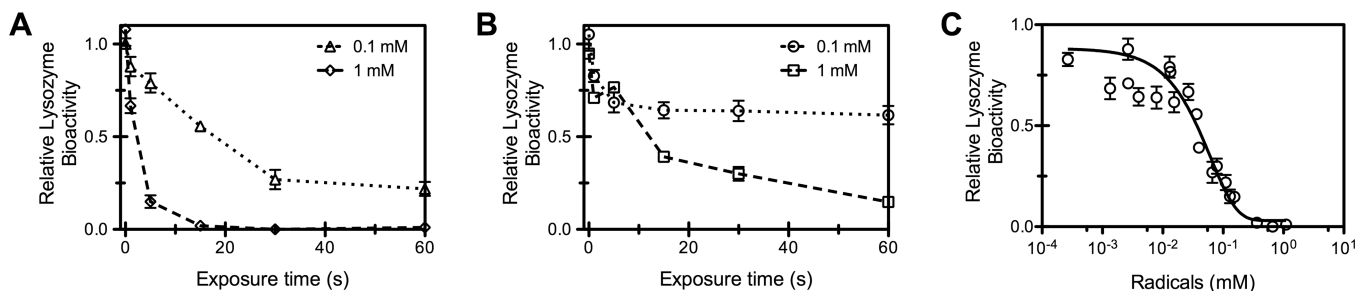


Figure 2. Protein destruction via photogenerated initiator radicals. Solutions of protein and LAP were exposed to light for various times and subsequently assayed for bioactivity relative to native protein. (A) Loss of bioactivity in the presence of 1 or 0.1 mM LAP, exposed to $I_0 = 10$ mW/cm² of 365 nm light for various times; (B) Loss of bioactivity for identical exposure times, but at a lower light intensity of 1 mW/cm²; (C) Loss of protein activity data plotted versus total concentration of radicals generated, with a trendline added for visualization. Loss of protein bioactivity was rapid above a critical radical concentration of ~0.002 mM.

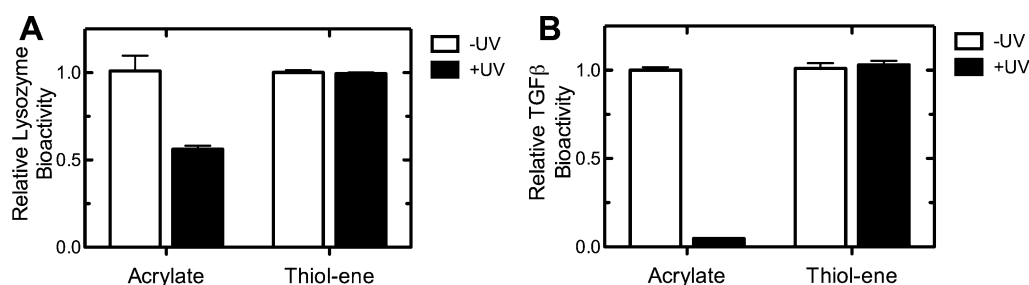


Figure 3. Loss of protein bioactivity upon exposure to photoinitiated radical species. Solutions of monomer, protein, and LAP (1 mM) were assayed for bioactivity before and after exposure to light at $I_0 = 10 \text{ mW/cm}^2$ ($\lambda = 365 \text{ nm}$). Acrylate and thiol-ene monomers, both at 40 mM functional group concentrations, were irradiated based on exposure times required for full shear modulus development. (A) For the acrylate reaction (180 s), lysozyme destruction is approximately 50%, while the thiol-ene step-growth reaction (10 s) preserves 100% of protein activity. Results are presented as average activity \pm sem ($n = 5$). (B) After exposure to the acrylate chain-growth reaction, TGF β loses all bioactivity, as measured by a reporter cell assay, while the thiol-ene step-growth reaction preserves 100% of protein activity. Results are presented as average activity \pm sem ($n = 4$).

monofunctional thiol. Relative protein bioactivity was measured for monomer/protein systems with no UV exposure, and compared to that of a native protein solution (Figure 3A.) Both acrylate and thiol-ene monomer solutions, each with a LAP concentration of 1 mM, were then exposed to light ($I_0 = 10 \text{ mW/cm}^2$, $\lambda = 365 \text{ nm}$). Exposure times from Table 1 were used to mimic the total number of radicals generated during photoinitiation that are required for full network development of the target hydrogel formulations. It should be noted that these solutions were exposed to light in optically thin conditions and that, for 365 nm light at $I_0 = 10 \text{ mW/cm}^2$, more than 180 s are required to completely consume the initial LAP. Lysozyme exposed to acrylate chain growth (180 s) exhibits a 50% reduction in bioactivity relative to a non-irradiated monomer solution. This result agrees well with previously published work^{17,18} showing a “functional group protective effect.” Namely, the higher concentration of reactive groups relative to protein concentration, typically a difference of several orders of magnitude, provides limited protection to proteins present in situ during polymerization.

Interestingly, the thiol-ene reaction significantly increased the recovery of bioactive protein; after 10 s of light dosage, the relative lysozyme bioactivity was identical to that of a solution receiving no light dose. We postulate that this protein protection may be due to two factors. First, the rapid conversion of the thiol-ene reaction allows for shorter light exposure times and a lower total number of radicals generated, as discussed previously. Second, protein protection may be afforded due to the reactivity of the propagating radical species itself. In a (meth)acrylate chain-growth reaction, a vinyl carbon radical is propagated, while in the thiol-ene step-growth mechanism, each propagation step results in both consumption and regeneration of a thiyl radical. Our findings suggest that these thiyl radical species may be less destructive to proteins in situ or that the thiol-ene reaction is less promiscuous than the (meth)acryl chain-growth mode of polymerization.

To confirm protein protection results with the model protein lysozyme, we devised a study to measure the relative protection afforded by the thiol-ene and acrylate reactions using a more biologically significant protein. The cytokine TGF β is implicated in a number of cellular processes, and like many signaling proteins, exhibits bioactivity at very low concentrations on the order of pico- to nanomolar.⁵⁰ TGF β was included in acrylate and thiol-ene monomer solutions at a concentration of 20 nM. As a control, TGF β /monomers were diluted in culture medium and incubated with a reporter cell

line (PE.25) for 18 h. Monomer/protein solutions were also exposed to light ($I_0 = 10 \text{ mW/cm}^2$, $\lambda = 365 \text{ nm}$) for times appropriate for gel cross-linking (Table 1) and subsequently diluted in culture medium. Following incubation, cells were lysed and the lysate assayed for luciferase activity, a measure of bioactive TGF β concentration in the medium (Figure 3B). Nonirradiated solutions of acrylate and thiol-ene monomers had a similar luciferase activity, indicating that the monomers had no innate effect on the cell reporter assay. Following polymerization, however, relative TGF β bioactivity was distinctly higher for proteins in the thiol-ene monomer formulations, while TGF β exposed to the acrylate chain-growth reaction retained no detectable bioactivity. This finding is in contrast to the results reported in Figure 3, where the acrylate polymerization resulted in only 50% loss of lysozyme activity. The higher damage could be due to differences in protein molecular weight (TGF β is 25 kDa, lysozyme is 15 kDa), susceptibility of the protein active site to radical damage, or concentration of protein in the photopolymerization. Biologically relevant protein concentrations were chosen for this study and for both lysozyme and TGF β . In either case, protein bioactivity was maintained at higher levels following exposure to thiol-ene reaction conditions.

Characterizing Protein Protection Afforded by the Thiol-ene System. To further characterize the ability to encapsulate proteins and maintain their activity using radically mediated thiol-ene polymerizations, we next conducted in situ protein/polymerization studies with varying concentration of a photoinitiator species, as this approach provides a facile method to study the effect of radical concentration on protein protection during a thiol-ene polymerization. Solutions of protein and monomer were prepared and the initiator LAP was included in the solutions at three different concentrations: 0.1, 1, and 10 mM. Protein solutions with no photoinitiator, both with and without thiol-ene monomer, were also prepared to determine loss of protein bioactivity, if any, due to irradiation alone. All protein solutions were exposed to light ($\lambda = 365 \text{ nm}$, $I_0 = 10 \text{ mW/cm}^2$) for a total of 60 s and subsequently assayed for protein bioactivity. Bioactivity results were normalized to a native protein sample and are presented in Figure 4. Native protein, in the absence of thiol-ene monomer and LAP, maintained $\sim 95\%$ of preirradiation activity, a result that indicates light exposure alone has minimal negative effect on the function of lysozyme. When thiol-ene monomer is added to a protein solution but no photoinitiator is present, bioactivity is $\sim 100\%$ following light exposure. Radical damage, however,

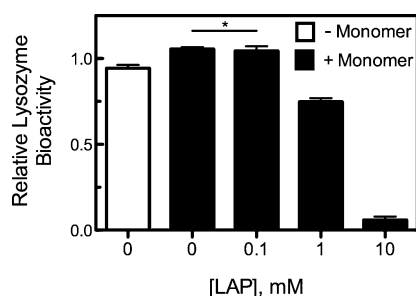


Figure 4. Protection of in situ protein bioactivity by thiol–ene monomer system. Thiol–ene photopolymerizations were initiated with varying concentrations of LAP, while reactive functional group and protein concentrations were held constant. Solutions were exposed to an identical light dosage ($I_0 = 10 \text{ mW/cm}^2$, $\lambda = 365 \text{ nm}$) for 60 s and subsequently assayed for protein bioactivity relative to a native protein solution. Results are presented as an average activity $\pm \text{sem}$ ($n = 5$).

was determined to be the primary mode of protein inactivation, as seen in data for solutions containing LAP. At the lowest initiator concentration tested, 0.1 mM, protein activity was maintained at approximately 100%; there was no significant difference in relative bioactivity between monomer solutions with 0 or 0.1 mM LAP concentration ($p < 0.005$). At higher concentrations of LAP, however, protein protection provided by the thiol–ene polymerization became limited.

For protein–monomer solutions formulated with 1 mM photoinitiator, $\sim 75\%$ of preirradiation protein activity was maintained after polymerization; when the thiol–ene reaction was initiated using 10 mM LAP, only 10% of protein activity remained following light exposure. This loss of protein protection by the thiol–ene system was somewhat expected, when considering the 60 s light dosage. For polymerization at $I_0 = 10 \text{ mW cm}^2$ ($\lambda = 365 \text{ nm}$), 60 s far exceeds the time required to fully form a cross-linked hydrogel material, as reported in Table 1. Based on this data, we hypothesized that the protection of proteins in situ during a thiol–ene polymerization was due, in part, to the presence of unreacted monomer functional groups. Thus, for the lower 0.1 mM LAP concentration, no loss of protein activity was observed over a 60 s exposure time, because this is the time scale over which polymerization occurs (i.e., the shear modulus is fully developed). For the same functional group concentration and light dosage, both 1 and 10 mM LAP concentrations fully form

a hydrogel in less than 10 s. Irradiation times beyond that necessary to reach complete polymerization would then result in radical generation in the absence of reactive groups, allowing proteins to be the primary target for radicals. In practical terms, this reinforces the importance of limiting overexposure in photocuring applications. Our hypothesis is supported by the data presented in Figure 4; however, to more fully characterize the time scale for protein destruction in the presence of a thiol–ene reaction, we designed a study to evaluate the light dosage conditions for in situ protein–polymer reactions and monitor resulting changes in bioactivity.

Effects of Varying Light Dosage on Protein Destruction During Thiol–Ene Polymerization. Solutions were prepared with a constant concentration of thiol–ene functional groups (40 mM) and lysozyme (1 μM), and these solutions were exposed to light ($I_0 = 10 \text{ mW cm}^2$, $\lambda = 365 \text{ nm}$) for a range of times from 0 to 180 s. Following photopolymerization, relative bioactivity of the protein in the reaction mixture was assayed and reported relative to a native protein solution. Results are plotted in Figure 5A. While the lower LAP concentration of 0.1 mM should exhibit the lowest protein destruction, results were somewhat unexpected. Over a 3 min exposure time, there was no effective change in lysozyme bioactivity, although this time exceeds what is required for complete polymerization and network formation. Likewise, when the thiol–ene polymerization was initiated with 10 mM LAP, solutions maintained high protein bioactivity. After 180 s of exposure, protein in the thiol–ene monomer system retains only 30% of preirradiation activity. These exposure times are much longer than that required to fully form a cross-linked hydrogel (Table 1), and this finding suggests that radical protection is afforded through a mechanism more complicated than that of simple functional group conversion.

Figure 5B shows relative protein activity when exposed to both 0.1 and 10 mM LAP photoinitiation conditions, plotted as a function of total radical generation. Results are plotted and fitted with a trendline, similar to the approach in Figure 2C with primary radicals. Interestingly, we observe that, in the presence of thiol–ene polymerization, protein protection is much higher, as observed by modest losses in protein activity occurring below a critical total generated radical concentration of 2.5 mM. This represents an increase of 3 orders of magnitude in activity relative to native protein solutions exposed to photoinitiator radicals in the absence of monomers

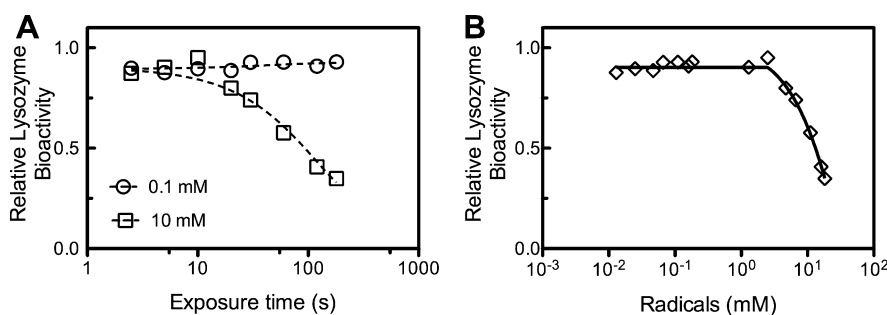


Figure 5. Loss in protein activity during photoinitiated radical generation with 0.1 and 10 mM LAP, following exposure to various light doses. Nongelling thiol–ene photopolymerizations were initiated with either 0.1 or 10 mM LAP, while functional group and protein concentrations were held constant. Solutions were exposed to light ($I_0 = 10 \text{ mW/cm}^2$, $\lambda = 365 \text{ nm}$) for 0, 2.5, 5, 10, 20, 30, 60, 120, and 180 s, and subsequently assayed for protein bioactivity. (A) Protein bioactivity after light exposure is plotted for 0.1 and 10 mM initiator as a function of light exposure time. (B) Protein bioactivity data is plotted as a function of total radical concentration. The line is included as a guide to the eye. Plateau extends to a radical concentration of 2.5 mM. Results are plotted as average activity $\pm \text{sem}$ ($n = 4$); error bars are smaller than the plotted symbols.

(Figure 2C). It is also noteworthy that this critical radical concentration for the onset in loss of protein activity is significantly higher than the radical number required to form hydrogels with 0.1, 1, or 10 mM LAP initiator.

Encapsulation and Recovery of Proteins from Cross-Linked Thiol–Ene Hydrogels. To demonstrate the utility of the thiol–ene reaction to recover proteins from PEG hydrogels, a number of proteins of various molecular weights were encapsulated in gels formed from 4-arm PEG norbornene and linear PEG dithiol (Table 2). LAP (1 mM) was used to initiate

Table 2. Protein Recovery from Cross-Linked Thiol–Ene Hydrogels^a

protein	molecular weight (kDa)	% recovery \pm SD
lysozyme	15	80.5 \pm 8.1
chymotrypsinogen	25	77.9 \pm 2.6
collagenase 3	60	91.7 \pm 14.7
bovine serum albumin	66	47.3 \pm 4.2
human serum		79.7 \pm 3.9

^aVarious proteins were encapsulated in thiol–ene hydrogels and release was monitored over a 24 h period. Results are presented as average \pm standard deviation ($n = 3$).

the photopolymerization ($I_0 = 10 \text{ mW/cm}^2$, $\lambda = 365 \text{ nm}$) for 5 s (i.e., the time required to fully form the gel). Protein-loaded gels were placed in PBS for 24 h, at which time the protein concentration that diffused into the supernatant was quantified. Recoveries of greater than 80% were measured for all encapsulated proteins, with the exception of bovine serum albumin (BSA). Interestingly, serum albumin has one non-oxidized cysteine residue that results in a free thiol,⁵¹ which may explain its low recovery. Finally, to assess the bioactivity of proteins encapsulated using thiol–ene gel systems, TGF β was studied. Specifically, TGF β was included at 20 nM in a monomer solution of 4-arm PEG norbornene and linear PEG dithiol using photopolymerization conditions that lead to high protein stability (Figure 3). Nonphotopolymerized monomer was added directly to culture medium. For comparison, the monomer/protein formulation was also photopolymerized ($I_0 = 10 \text{ mW/cm}^2$, $\lambda = 365 \text{ nm}$) for 10 s (i.e., the time required to fully form the gel (Table 1)), and the resulting hydrogel was added to the culture medium. Both media samples were then incubated with the PE.25 reporter cell line overnight, and cell lysate was assayed for luciferase activity. Results are plotted in Figure 6, showing that TGF β encapsulated via a thiol–ene reaction had nearly identical bioactivity to that of growth factor that was simply in solution but never exposed to the radical-mediated thiol–ene polymerization.

CONCLUSIONS

Hydrogels were formed via photopolymerization using acrylate chain-growth and thiol–ene step growth mechanisms, and the appropriate light doses were confirmed using in situ rheology under UV exposure. Loss of protein bioactivity following exposure to photogenerated primary radicals was characterized using the enzyme lysozyme. Nongelling solution polymerizations were then used to study loss of protein function during exposure to acrylate and thiol–ene photopolymerization reactions, using lysozyme and the cytokine TGF β . While the acrylate reaction provided some marginal protection to in situ protein, there was no loss of protein bioactivity following exposure to the thiol–ene reaction. This may be due to the

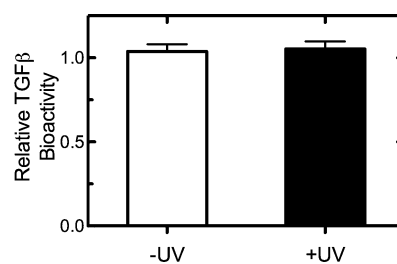


Figure 6. Encapsulation and recovery of bioactive TGF β from thiol–ene hydrogels. Solutions of monomer, TGF β , and LAP (1 mM) were assayed for bioactivity before and after light dosage ($I_0 = 10 \text{ mW/cm}^2$, $\lambda = 365 \text{ nm}$, 10 s). Solutions of 4-arm PEG norbornene/PEG dithiol, both at 40 mM functional group concentration, were added directly to culture medium (–UV) or were irradiated for times appropriate to fully form hydrogels (+UV). For cross-linked samples, the resulting polymer was swollen overnight in culture medium and incubated with PE.25 reporter cells. Cell lysate was assayed for luciferase activity to quantify bioactive TGF β concentration.

more rapid kinetics of the thiol–norbornene reaction or oxygen inhibition in the acrylate reaction, which required higher radical concentrations to proceed to completion. When lysozyme, chymotrypsinogen, collagenase, bovine serum albumin, human serum, and TGF β were encapsulated in cross-linked thiol–ene gels and subsequently released into PBS buffer, greater than 80% recovery was observed. Finally, TGF β was encapsulated in PEG hydrogels formed via a thiol–ene reaction, and no statistically significant loss of bioactivity was detected relative to the nonencapsulated growth factor. Photopolymerization reactions that provide rapid gelation at low radical concentrations are highly desirable for applications that seek to encapsulate sensitive payloads, such as proteins or cells. Results of this study indicate that thiol–ene click reactions are capable of proceeding rapidly at low initiator concentrations with little to no impact on in situ protein bioactivity.

AUTHOR INFORMATION

Corresponding Author

*E-mail: kristi.anseth@colorado.edu.

Notes

The authors declare no competing financial interest.

ACKNOWLEDGMENTS

The authors would like to thank Dr. Malar Azagarsamy and Kelly Trowbridge for assistance in manuscript preparation. PE.25 cells were a kind gift from Dr. Xuedong Liu from the Department of Biochemistry at the University of Colorado at Boulder. This research was funded in part by NIH R01 DE016523 and the Howard Hughes Medical Institute.

REFERENCES

- (1) Magin, C. M.; Finlay, J. A.; Clay, G.; Callow, M. E.; Callow, J. A.; Brennan, A. B. *Biomacromolecules* **2011**, *12* (4), 915–922.
- (2) Ju, H.; McCloskey, B. D.; Sagle, A. C.; Wu, Y. H.; Kusuma, V. A.; Freeman, B. D. *J. Membr. Sci.* **2008**, *307* (2), 260–267.
- (3) Caldorera-Moore, M.; Peppas, N. A. *Adv. Drug Delivery Rev.* **2009**, *61* (15), 1391–1401.
- (4) Griffith, L. G. *Acta Mater.* **2000**, *48* (1), 263–277.
- (5) Lin, C. C.; Metters, A. T. *Adv. Drug Delivery Rev.* **2006**, *58* (12–13), 1379–1408.
- (6) Pisal, D. S.; Kosloski, M. P.; Balu-Iyer, S. V. *J. Pharm. Sci.* **2010**, *99* (6), 2557–2575.

- (7) Tibbitt, M. W.; Han, B. W.; Kloxin, A. M.; Anseth, K. S. *J. Biomed. Mater. Res., Part A* **2012**.
- (8) West, J. L.; Hubbell, J. A. *Macromolecules* **1999**, *32* (1), 241–244.
- (9) Nuttelman, C. R.; Tripodi, M. C.; Anseth, K. *Matrix Biol.* **2005**, *24* (3), 208–218.
- (10) Fairbanks, B. D.; Schwartz, M. P.; Halevi, A. E.; Nuttelman, C. R.; Bowman, C. N.; Anseth, K. S. *Adv. Mater.* **2009**, *21* (48), 5005–5010.
- (11) Yang, Z. H.; Galloway, J. A.; Yu, H. U. *Langmuir* **1999**, *15* (24), 8405–8411.
- (12) Kingshott, P.; McArthur, S.; Thissen, H.; Castner, D. G.; Griesser, H. J. *Biomaterials* **2002**, *23* (24), 4775–4785.
- (13) Fairbanks, B. D.; Schwartz, M. P.; Bowman, C. N.; Anseth, K. S. *Biomaterials* **2009**, *30* (35), 6702–6707.
- (14) Bryant, S. J.; Nuttelman, C. R.; Anseth, K. S. *J. Biomater. Sci., Polym. Ed.* **2000**, *11* (5), 439–457.
- (15) Kim, I. L.; Mauck, R. L.; Burdick, J. A. *Biomaterials* **2011**, *32* (34), 8771–8782.
- (16) Sabnis, A.; Rahimi, M.; Chapman, C.; Nguyen, K. T. *J. Biomed. Mater. Res., Part A* **2009**, *91A* (1), 52–59.
- (17) Lin, C. C.; Sawicki, S. M.; Metters, A. T. *Biomacromolecules* **2008**, *9* (1), 75–83.
- (18) McCall, J. D.; Lin, C. C.; Anseth, K. S. *Biomacromolecules* **2011**, *12* (4), 1051–1057.
- (19) Anseth, K. S.; Wang, C. M.; Bowman, C. N. *Polymer* **1994**, *35* (15), 3243–3250.
- (20) Johnson, L. M.; Fairbanks, B. D.; Anseth, K. S.; Bowman, C. N. *Biomacromolecules* **2009**, *10* (11), 3114–3121.
- (21) Quick, D. J.; Anseth, K. S. *Pharm. Res.* **2003**, *20* (11), 1730–1737.
- (22) Quick, D. J.; Anseth, K. S. *J. Controlled Release* **2004**, *96* (2), 341–351.
- (23) Berchtold, K. A.; Lovell, L. G.; Nie, J.; Hacıoglu, B.; Bowman, C. N. *Polymer* **2001**, *42* (11), 4925–4929.
- (24) Pilkenton, M.; Lewman, J.; Chartoff, R. *J. Appl. Polym. Sci.* **2011**, *119* (4), 2359–2370.
- (25) Decker, C.; Jenkins, A. D. *Macromolecules* **1985**, *18* (6), 1241–1244.
- (26) Elias, R. J.; McClements, D. J.; Decker, E. A. *J. Agric. Food Chem.* **2005**, *53* (26), 10248–10253.
- (27) Gebicki, S.; Gebicki, J. M. *Biochem. J.* **1993**, *289*, 743–749.
- (28) Elias, R. J.; Kellerby, S. S.; Decker, E. A. *Crit. Rev. Food Sci. Nutr.* **2008**, *48* (5), 430–441.
- (29) Marx, G.; Chevion, M. *Biochem. J.* **1986**, *236* (2), 397–400.
- (30) Bowman, C. N.; Hoyle, C. E. *Angew. Chem., Int. Ed.* **2010**, *49* (9), 1540–1573.
- (31) Yang, M. Q.; Mao, J.; Nie, W.; Dong, Z. X.; Wang, D. P.; Zhao, Z. L.; Ji, X. L. *J. Polym. Sci., Part A* **2012**, *50* (10), 2075–2083.
- (32) Chen, R. T.; Marchesan, S.; Evans, R. A.; Styan, K. E.; Such, G. K.; Postma, A.; McLean, K. M.; Muir, B. W.; Caruso, F. *Biomacromolecules* **2012**, *13* (3), 889–895.
- (33) Lluch, C.; Ronda, J. C.; Galia, M.; Lligadas, G.; Cadiz, V. *Biomacromolecules* **2010**, *11* (6), 1646–1653.
- (34) Lin, C. C.; Raza, A.; Shih, H. *Biomaterials* **2011**, *32* (36), 9685–9695.
- (35) Anderson, S. B.; Lin, C. C.; Kuntzler, D. V.; Anseth, K. S. *Biomaterials* **2011**, *32* (14), 3564–3574.
- (36) Benton, J. A.; Fairbanks, B. D.; Anseth, K. S. *Biomaterials* **2009**, *30* (34), 6593–6603.
- (37) Aimetti, A. A.; Machen, A. J.; Anseth, K. S. *Biomaterials* **2009**, *30* (30), 6048–6054.
- (38) Scott, T. F.; Cook, W. D.; Forsythe, J. S.; Bowman, C. N.; Berchtold, K. A. *Macromolecules* **2003**, *36* (16), 6066–6074.
- (39) Berchtold, K. A.; Randolph, T. W.; Bowman, C. N. *Abstr. Pap. ACS* **2003**, *225*, U680–U680.
- (40) Anseth, K. S.; Wang, C. M.; Bowman, C. N. *Macromolecules* **1994**, *27* (3), 650–655.
- (41) Baldwin, S. P.; Saltzman, W. M. *Adv. Drug Delivery Rev.* **1998**, *33* (1–2), 71–86.
- (42) Clarke, D. C.; Brown, M. L.; Erickson, R. A.; Shi, Y. G.; Liu, X. *D. Mol. Cell. Biol.* **2009**, *29* (9), 2443–2455.
- (43) Wang, J.; Ugaz, V. M. *Electrophoresis* **2006**, *27* (17), 3349–3358.
- (44) Cook, W. D.; Chausson, S.; Chen, F.; Le Pluart, L.; Bowman, C. N.; Scott, T. F. *Polym. Int.* **2008**, *57* (3), 469–478.
- (45) He, H. Y.; Li, L.; Lee, L. J. *React. Funct. Polym.* **2008**, *68* (1), 103–113.
- (46) Reddy, S. K.; Cramer, N. B.; Bowman, C. N. *Macromolecules* **2006**, *39* (10), 3673–3680.
- (47) Odian, G. G. *Principles of Polymerization*, 4th ed.; Wiley: Hoboken, NJ, 2004; p xxiv, 812 p.
- (48) Avens, H. J.; Bowman, C. N. *J. Polym. Sci., Part A* **2009**, *47* (22), 6083–6094.
- (49) Gou, L. J.; Coretsopoulos, C. N.; Scranton, A. B. *J. Polym. Sci., Part A* **2004**, *42* (5), 1285–1292.
- (50) Tayalia, P.; Mooney, D. J. *Adv. Mater.* **2009**, *21* (32–33), 3269–3285.
- (51) He, X. M.; Carter, D. C. *Nature* **1992**, *358* (6383), 209–215.